Assessment and improvement of modeling the atmospheric attenuation based on aerosol optical depth information with applicability to solar tower plants

Jesús Polo [1*], Jesús Ballestrín[2], Elena Carra[2]

[1] Photovoltaic Solar Energy Unit (Renewable Energy Division, CIEMAT), Avda. Complutense 40, 28040 Madrid, Spain
[2] Solar Concentrating Systems Unit, (PSA, CIEMAT), 04200 Almería, Spain

* Corresponding author
Jesús Polo, email: jesus.polo@ciemat.es, Phone: +34 914962513, Fax : +34 913466037

Abstract

Accurate modeling of atmospheric attenuation phenomena is a crucial aspect for the performance of solar tower plants. The development of suitable models requires of reliable measurements of the extinction coefficient near surface. Continuous monitoring of the extinction coefficient at ground is being recorded at Plataforma Solar de Almería (PSA) facility in south-east Spain since July 2017 offering a unique and long experimental database for model assessment. This work presents the assessment of Polo's model with over two years of ground measurements. In addition, a new corrected and improved version of the model is presented here with a very good performance, maintaining the versatility of the model. Hourly estimations of the atmospheric attenuation at PSA with the new version of the model resulted in a 6.1% of RMSE and very good agreements in both inter- and intra-annual variability is found. The new model proposed here is easy to be used in both ray-tracing, optimization software and performance tools commonly and widely used for modeling solar tower plants behavior and production. This new model offers a better and novel approach that can be used at any site where AOD information is available.

Keywords: central receiver; atmospheric attenuation; optical losses; solar tower plants modeling; concentrating solar power; solar resource

1. Introduction

Central receiver technologies, particularly molten salt tower plants, have been gaining interest and prominence in the concentrating solar power (CSP) industry. The large thermal storage capacity and high working temperatures at the receiver are the great attractions of this kind of plants. Current and future perspectives of CSP technologies and developments, including solar

tower projects, can be found extensively in the information provided by SolarPACES programme from the International Energy Agency (https://www.solarpaces.org/).

The solar field of a solar tower plant consists of a very large number of mirrors (heliostats) tracking the Sun's position in the sky and reflecting the solar direct radiation to the receiver placed in the upper part of the tower. The image of the solar flux on the receiver is affected by the optical losses taking place in the solar field, which include cosine loss, shadowing and blocking, spillage and atmospheric attenuation [1]. In order to minimize most of the negative effects of the optical losses, optimization algorithms have been developed for effective designing of the solar field [2–4]. The atmospheric attenuation is due to scattering and absorption processes that take place in the optical path between the heliostats and the receiver, known as slant range, and depends on the turbidity conditions in the atmospheric boundary layer (the bottom layer of the atmosphere in the order of the tower height). Thus, the optical losses due to atmospheric attenuation may produce a significant reduction of the optical efficiency of plants with a large solar field (large power output) in desert or semi-arid climates [5].

Different methodologies have been proposed in the recent years for measuring the atmospheric attenuation on ground [6–10]. Ballestrin et al. proposed an innovative measuring system based on two cameras of very high resolution facing a lambertian target [6]. The same team reported intra-annual analysis of extinction after one year of measurements [10]. Hanrieder at al. developed a measuring technique by combining a scatterometer and a visibility transmissometer [7]. More recently Hanrieder et al. reported a methodology for determining the atmospheric attenuation based only on direct normal irradiance (DNI) measurements [9]. Sanchez et al. presented recently another method by using reflector telescopes [8]. However, only the measuring system ta PSA has provided rather continuous and long measurements of the extinction near ground.

On the other hand, several methodologies have been also proposed for modeling the atmospheric attenuation [11–17]. Sengupta et al. proposed a simple transmittance model based on DNI [16] which was further reviewed and enhanced by Hanrieder et al. [13]. Another model based on DNI and Beer-Lambert equation was also proposed by Tahboud et al. [17]. Radiative transfer computations have given rise to other formulations. Polo et al. proposed a model based on multiple radiative transfer computations that formulate the atmospheric attenuation as a function of the AOD and the slant path [14]. In addition, a thorough study on the impact of the time resolution of AOD input information and the impact on plant performance was further highlighted [15]. In addition the use of satellite-derived AOD information for modeling the extinction was also explored by Carra et al. [11]. A thorough review on both measuring and modeling atmospheric attenuation including the initial studies in the late seventies can be found in the recent literature [18].

The measurement of the attenuation and the extinction coefficient at the atmospheric boundary layer has been addressed at PSA under the PRESOL project by using two simultaneous images of a proper target at a representative slant range [6,19]. Continuous monitoring of the attenuation between two cameras is being carrying out since July 2017; nevertheless, maintenance and other actuations on the measurement system have resulted in few gaps in the experimental database. Local extinction coefficient is then derived from the atmospheric attenuation corresponding to the slant range of the PSA experimental system. The availability of such a long experimental database allows the assessment, validation and improving of models developed during the PRESOL project for accurate estimation the atmospheric attenuation [14,15]. This work presents the validation of the Polo's model and a new improved version based on incorporating characteristics of the distribution function of

observations. The improved version of the model is able to estimate the local atmospheric attenuation in hourly basis with a 6.1% of RMSE using as input the aerosol optical depth (AOD) at 550 nm.

The novelty of this work is remarked by the unique characteristics of the experimental database on atmospheric attenuation that is monitoring accurately and continuously the extinction near ground for more than two years; these measurements in south-east Spain are also representative of proper climatic conditions for solar tower plants (arid climates with high direct normal solar irradiation). In addition, the long experimental database is very adequate for evaluating and developing reliable models for computing the atmospheric attenuation. The model proposed here is then proven to permit an accurate estimation of the attenuation since the relationship between column AOD and near surface extinction has been accurately fitted with the help of experimental measurements. Finally, the new improved model allows dynamic modeling of attenuation with applications to central receiver technologies because the dependence with the AOD, proposed and characterized in this work, make suitable its use in solar tower modeling tools and it can be used universally as long as reliable data on AOD be available.

2. Experimental data

A novel and reliable method for continuous measuring the atmospheric attenuation was proposed by CIEMAT researchers and set up at Plataforma Solar of Almeria (PSA). The measuring system consisted in the synchronized acquisition of images of a lambertian target by two high-resolution digital cameras placed approximately at 83 and 825 m, respectively [6,19]. A topographic study and a rigorous individual optic adjustment of each camera ensured the same target area with the same resolution for both cameras images. A thorough and detailed description of all the aspects and configuration of the measuring system at PSA can be found in the referenced literature [6]. The proper analysis of the two images at every acquisition instant produces a measurement of the extinction coefficient and, thus the atmospheric attenuation in percentage corresponding to the distance between cameras (742 m). Figure 1 shows a picture of PSA facilities and the position of the cameras and target. It should be remarked that both the distance and the operational spectral range of the cameras are representative experimental conditions of the phenomena under study in the framework of solar tower plants (the furthest heliostats in solar tower plants are in the range of 1 km). Thus the distance of 742 m is the slant range of the atmospheric attenuation phenomena being measured. The experimental facility is in operation since July 2017 so that there is a long database of measurements available that allow the characterization of intra and inter-annual variability of atmospheric attenuation at PSA [10].

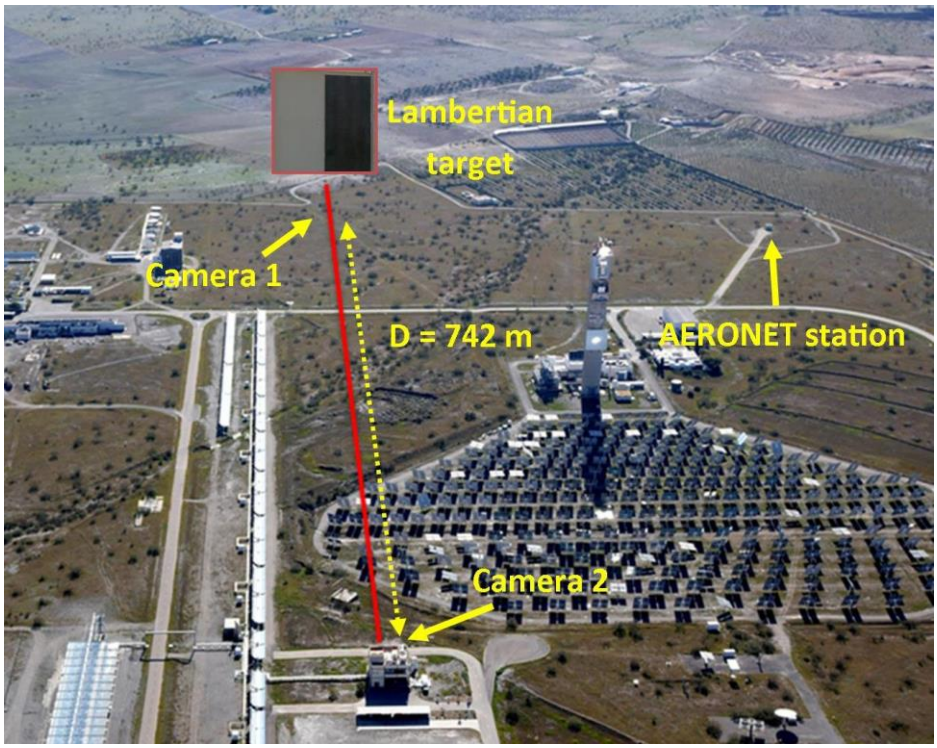

Figure 1. Experimental set up for measuring atmospheric attenuation at PSA.

The light extinction taking place along the distance D can be obtained by the difference of intensity between two simultaneous images. The atmospheric attenuation as a function of the effective intensity of each image is defined by,

$$A(\%) = 100\left(1 - \frac{I_2}{I_1}\right) \quad (1)$$

Where I_1 and I_2 are the effective intensities of the images corresponding to camera 1 and 2, respectively. The lambertian target is divided in two areas of the same size, one painted in white Amercoat® 741 and the other in black Zynolyte®, to ensure highly reflective and absorbed surfaces, respectively. Therefore, the effective intensity of camera i is determined by the difference between white (I_{iW}) and black (I_{iB}) sides of the lambertian target,

$$I_i = I_{iW} - I_{iB} \quad (2)$$

This is an effective way to remove the scattered light from the surroundings that could be received by each camera and ensure that the cameras only accounted for the reflected light from the target.

In addition to the atmospheric attenuation measurements, an AERONET station is also placed at PSA site, named Tabernas PSA-DLR station (Figure 1). AERONET is an extensive network of ground stations providing accurate measurements of AOD, and other parameters for optical characterization of atmospheric aerosols, from spectral direct normal irradiance measurements with sunphotometers [20,21]. AOD level 2.0 data (cloud-screened and quality controlled), with the inversion direct sun algorithm version 3 [22,23], from this station has been collected for the period 2017-2019. Nominal standard aerosol wavelengths are 340, 380, 440, 500, 675, 870, 1020 and 1640 nm [23]. Following the Angstrom equation for the AOD dependence with the wavelength, AOD 550 nm data have been obtained by linear interpolation from the two nearest wavelengths in logarithm scale (AOD 500 nm and AOD 675 nm). The wavelength dependence of the Angstrom exponent can be better described by a second-order polynomial empirical relationship between the logarithmic AOD and logarithmic wavelengths [24]. However the curvature in that relationship depends on the aerosol type and for coarse mode dominated aerosols (associated with dust and sea salt) the linear interpolation can be used without significant error [25].

Figure 2 shows the raw data of both atmospheric attenuation and AOD 550 nm, hereafter AOD, collected from the extinction measuring system and AERONET station at PSA for the period 2017-2019. A clear direct correlation can be observed between both parameters.

The collected AOD measurements of Tabernas PSA-DLR station have a sampling time around 10 minutes and there are gaps in the experimental database. On the other hand, the attenuation measurements in the PSA experimental system started with 15-minute sampling from 11:00 to 14:00 and they were extended to 1-minute basis with a time window of 10:00-15:00 every day. Therefore, there are no simultaneous and perfectly matched values in the instantaneous measurements of both AOD and attenuation measurements.

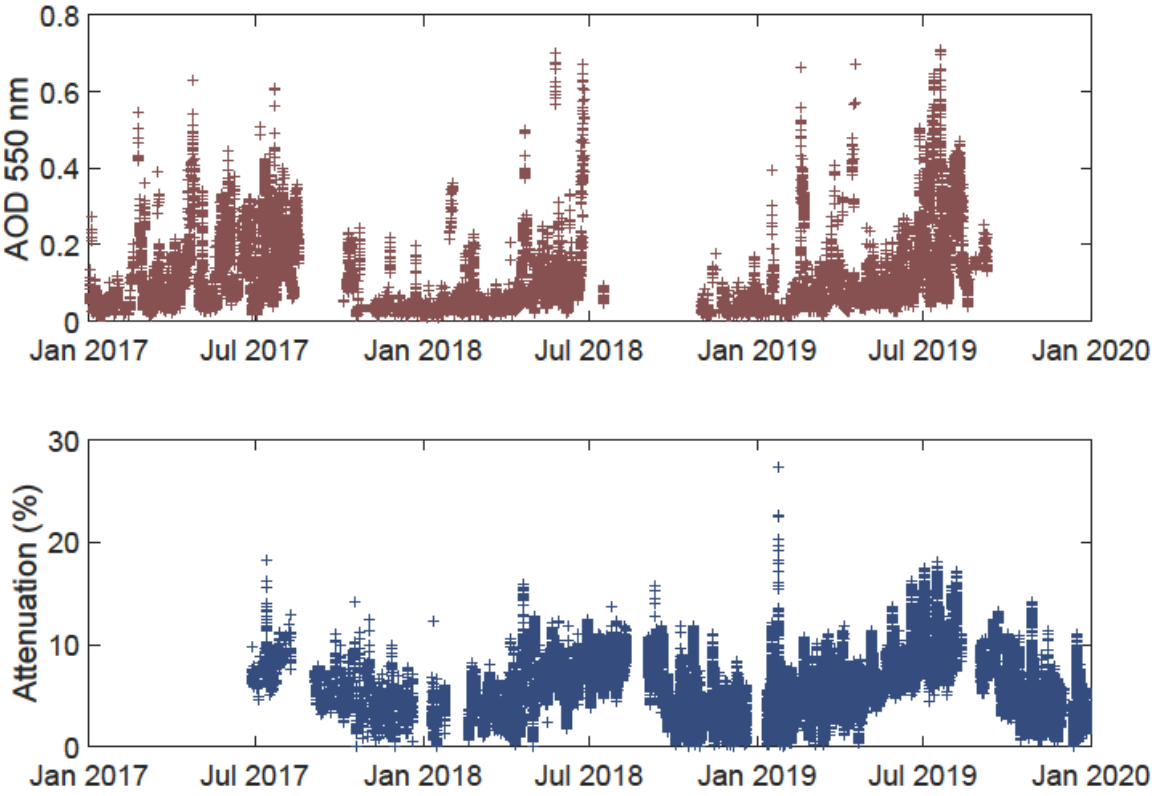

Figure 2. AOD and atmospheric attenuation measurements collected at PSA for the period 2017-2019.

3. Modeling

The model to assess and validate in this work was proposed from extensive radiative transfer calculations with libRadTran code [26–28] covering a wide range of AOD values and slant ranges [14]. The Polo et al. model was designed as a functional model that could be expressed in a polynomial form and with parametric dependence on both AOD and slant path in order to be used at any site where AOD information was available. Therefore, an analysis of the range of variability of AOD 550 nm was performed using all the AERONET ground stations, selecting finally the AOD ranges from 0.06 to 0.72 [14]. Radiative transfer calculations where performed on the AOD variability and on different slant paths ranging from 150 m to 3 km to create a database of computed attenuation that could be fitted to a polynomial function.

The Polo et al. model calculates the atmospheric attenuation in percentage assuming a third order polynomial function of the slant range (expressed in km),

$$A(\%) = a\,S^3 + b\,S^2 + c\,S + d \tag{3}$$

The polynomial coefficients have a functional dependence on the AOD, which is the explicative variable of the attenuation variability in the model. Using the data from the multiple radiative transfer calculations for the different slant paths and AOD values third order polynomial expressions where fitted for the coefficients as a function of the AOD [14].

$$\begin{aligned} a &= 3.13\,AOD^3 - 1.96\,AOD^2 + 1.60\,AOD - 0.133 \\ b &= -14.74\,AOD^3 + 2.49\,AOD^2 - 11.85\,AOD + 0.544 \\ c &= 28.32\,AOD^3 - 7.57\,AOD^2 + 48.74\,AOD + 0.371 \\ d &= -2.61\,AOD^3 + 3.70\,AOD^2 - 2.64\,AOD + 0.179 \end{aligned} \tag{4}$$

Modeling the atmospheric attenuation by a third order polynomial seems to be a convenient and versatile approach due to: 1) the third order polynomial function fits quite well the attenuation dependence with the slant range observed in many studies [29,30], 2) most ray-tracing tools and performance models have already implemented this polynomial functional form to estimate the atmospheric attenuation [31,32]. Therefore, in order to keep the polynomial function of the model the dependence with the AOD was formulated through the polynomial coefficients. The use of AOD as input parameter allows the model to have sensitivity to the dynamic behavior of the atmospheric boundary layer. AOD is accurately measured in many sites worldwide and, in addition, retrievals from reanalysis-based models and satellite are available as gridded data worldwide.

Even though the instantaneous AOD data do not overlap perfectly in time with the instantaneous attenuation measurements it is illustrative to estimate attenuation with this model using raw AOD data as input. Figure 3 shows the comparison of estimated and measured attenuation for the 3-year period. There are similarities in the behavior of modeled data with the AOD trend but an underestimation of the attenuation is generally observed in the model. The discrepancies are expected since the model formulates the sensitivity of the attenuation at a given distance as a function of AOD. The attenuation (perceived as extinction phenomena occurring in a nearly horizontal optical path) depends, in absence of very low clouds and fog, fundamentally on the turbidity or visibility conditions in the atmospheric boundary layer, i.e. the aerosol surface extinction coefficient. The AOD is the integral of the extinction coefficient along the entire atmospheric vertical column. The aerosol extinction coefficient decreases with the height, and thus since the AOD is the integration of the extinction coefficient along the vertical path, it is expected that AOD underestimates the extinction near ground; only under long stable atmospheric conditions the AOD could be a good estimation of the extinction near ground. Therefore, the knowledge of the relationship between the AOD and aerosol surface extinction coefficient requires a good determination of

the aerosol vertical distribution [33]. A two layer aerosol model with a well-mixed bottom layer and an upper layer with exponential decrease of aerosol extinction with the altitude has been recently proposed with good results [34]. Therefore, despite AOD and the extinction at the lower boundary layer are correlated, they may represent different attenuating conditions at the same time instants. Studies in the literature evaluating the representativeness of near-surface in situ measurements compared to the total atmospheric column has shown correlation, but also important bias between in situ and sun photometer measurements [35]. Recent works showed that aerosol extinction coefficients tends to be larger near the ground and thus surface extinction based on AOD would result in underestimating the actual attenuation [36]. The same authors proposed decreasing exponential functions of the AOD to better modeling the surface extinction coefficient [36]. The results of these recent studies are consistent with the bias and underestimation of modeling surface attenuation with vertical AOD observed in Figure 3.

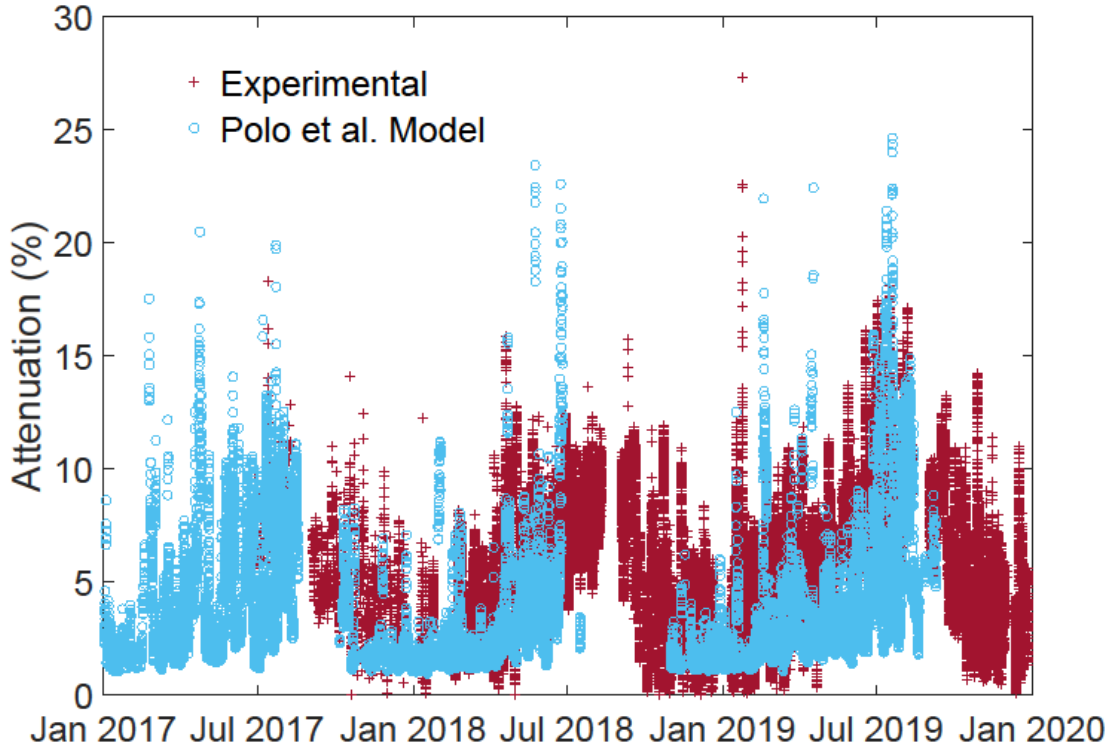

Figure 3. Assessment of Polo's model using raw AOD measurements.

4. Assessment and improvement of modeling

In order to have overlapped data on both measured AOD and attenuation level all the experimental data (attenuation measurements and AOD) have been aggregated in hourly, daily and monthly means. Modeling of hourly, daily and monthly attenuation was performed with the Polo's model. Figure 4 shows, in the upper plot, the scatter plot of the modeled versus experimental hourly data, and in the lower plot, the probability density functions (pdf) of experimental and modeled hourly data. Both plots indicate a trend to underestimate the hourly attenuation measured at PSA. In addition, the distribution functions of modeled and measured data show significant differences as a consequence of the bias. Mean bias error (MBE) and root mean squared error (RMSE) of hourly modeled attenuation are 1.6% and 10.9%, respectively. In order to correct and improve the model performance techniques based on correcting the distribution function of modeled data can be used. These kinds of techniques have been previously used in climatology analysis for correcting bias in modeling results with the use of the distribution function of observations.

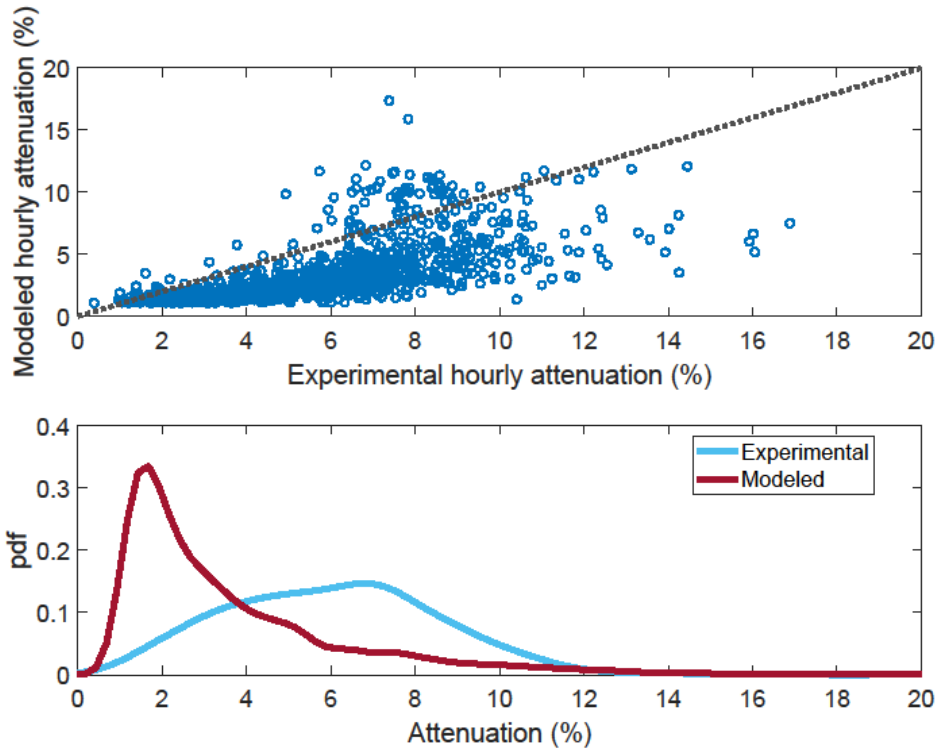

Figure 4. Assessment of Polo's model for hourly attenuation data.

The quantile mapping (QM) technique is frequently used in meteorology and climate modeling for correcting large bias modeled data. The technique makes use of the empirical distribution of the observations to correct the data. The cumulative distribution function (CDF) can be used as an operator to correct data in the quantile domain [37],

$$y_c = \mathrm{CDF}_o^{-1}[\mathrm{CDF}_m(x_m)] \tag{5}$$

where $\mathrm{CDF_o}$ and $\mathrm{CDF_m}$ are the cumulative distribution functions of the observed and modeled data, respectively, x_m are the modeled data and y_c are the new corrected modeled data. The quantiles of modeled and observed data can be computed by the full empirical non-parametric

distribution or by a fitted theoretical parametric distribution [38–40]. QM has been also used recently in improving solar radiation modeled datasets among other methodologies for site adaptation [41].

Using QM a new set of modeled attenuation data, in hourly basis, have been created whose distribution function fits the one of the experimental attenuation hourly data. Figure 5 shows the CDF of the uncorrected and corrected modeled attenuation compared with the CDF of the experimental data where the improvement of the new estimations is very remarkable.

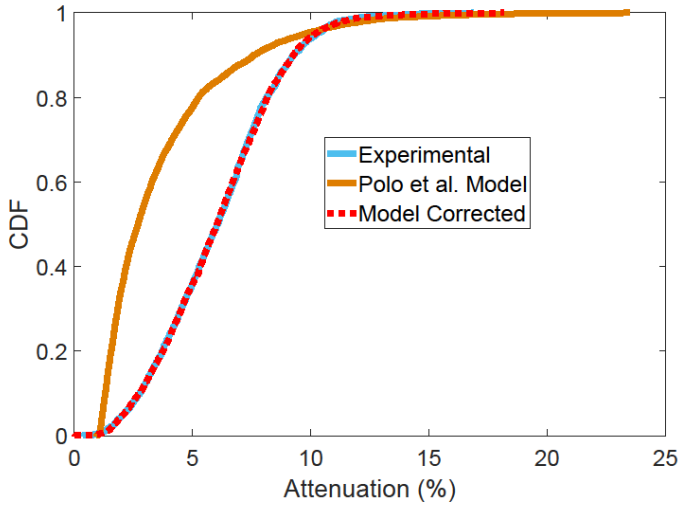

Figure 5. DF of modeled attenuation by Polo's model and by QM corrections.

The results of QM can be used for developing a correction factor to Polo's model that improves the performance and reduces the uncertainty of modeled attenuation. Let's define a correction factor f as the ratio of the corrected attenuation data resulted from QM to the original output of Polo's model. The values of f show a very interesting dependence with the AOD that can be very well fitted to piecewise exponential functions (Figure 6). The proposal of decreasing exponential function of the AOD is in agreement with recent studies for better modeling surface extinction coefficient [36].

$$f = \begin{cases} 2.874\, e^{-3.059\, AOD} - 7.445 e^{-114.7\, AOD} & AOD \leq 0.05 \\ 2.358\, e^{-7.094\, AOD} + 0.836 e^{-0.141\, AOD} & AOD > 0.05 \end{cases} \quad (6)$$

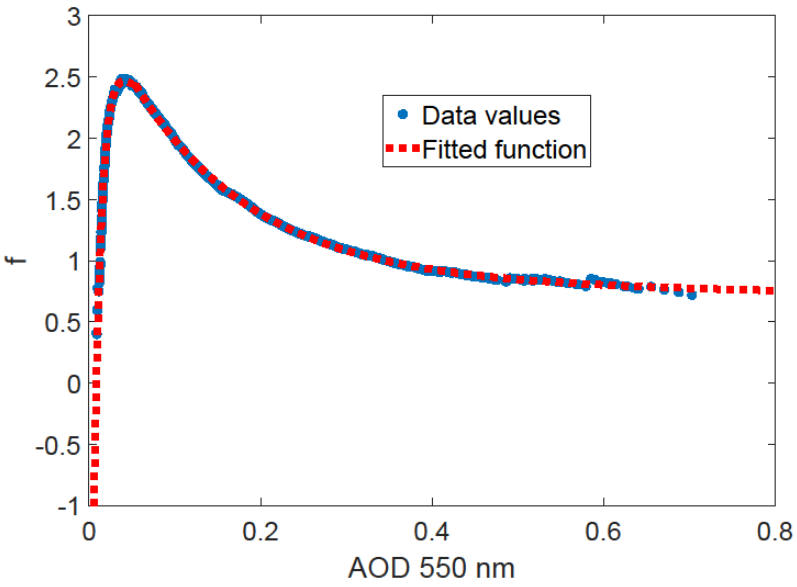

Figure 6. Correction factor for modeling attenuation as a function of AOD.

Therefore, the new version of the model consists of new polynomial coefficients that result from multiplying the actual ones (in equation 4) by the correction factor f. In other words, the modeled attenuation in equation 1 is multiplied by f to get the corrected attenuation in percentage. The corrected model has a better performance than the original one with a significant reduction of bias (MBE = -0.05%) and RMSE of 6.1% in the hourly estimations of the attenuation. Figure 7 shows the scatter plots of hourly, daily and monthly aggregates of estimated attenuation compared to the experimental observations. A high good performance can be observed in the scatter plots for all the aggregated data. Figure 8 shows the time series of aggregates corresponding to the experimental attenuation and the estimations by both the original and the corrected model. This plot shows also the good performance of the intra-annual trend. Therefore, the exponential function f in equation 6 corrects the systematic difference associated to the fact that AOD underestimate the extinction in the lower atmospheric layers due to the integral character of the AOD. Thus, the goodness of this improved model may have a positive techno-economic impact in the studies and analysis with performance models, like SAM [42,43], or optimization models for heliostat solar fields, like SoFIA [44].

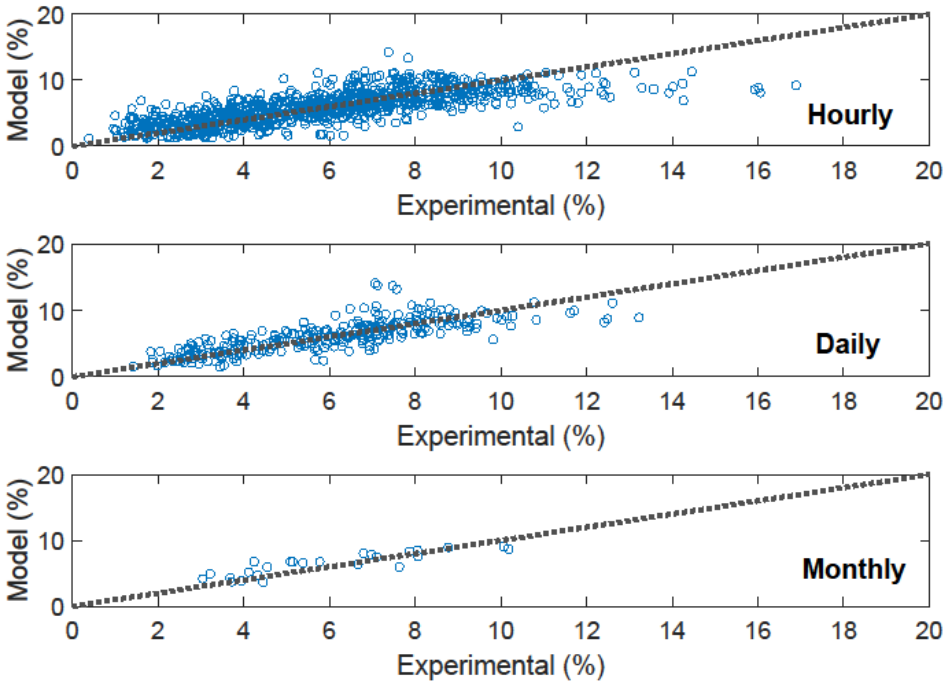

Figure 7. Scatter plot of corrected model for hourly, daily and monthly aggregates of atmospheric attenuation.

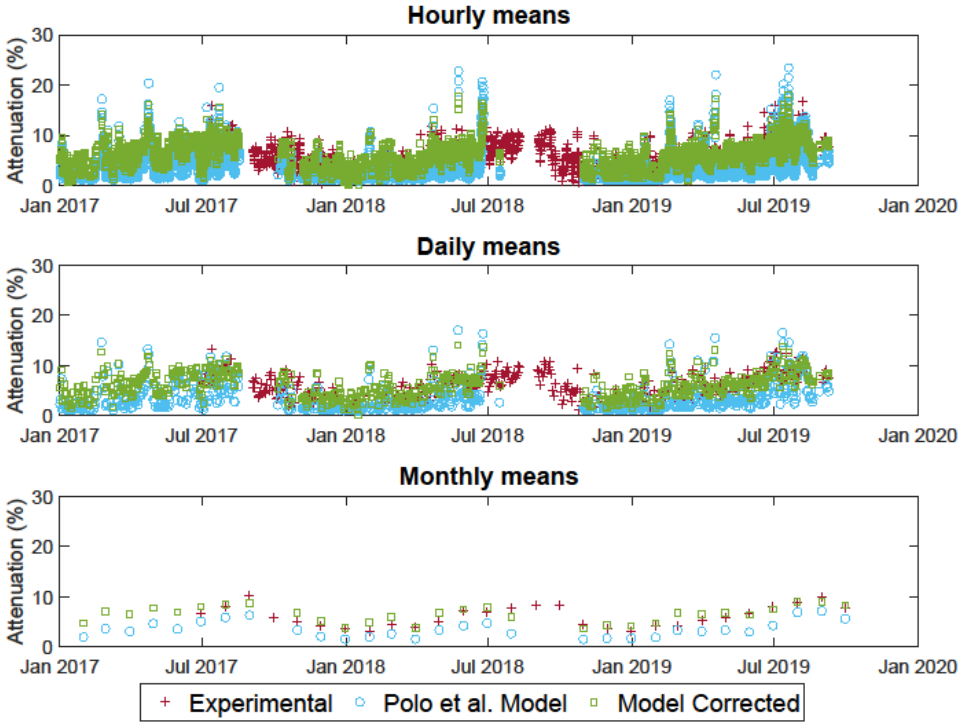

Figure 8. Time series of measured and estimated atmospheric attenuation in hourly, daily and monthly basis.

5. Conclusions

Atmospheric attenuation of reflected direct irradiance taking place between far heliostats and the receiver may play an important role in the optical losses of a solar tower plant. Large power plants involve towers around 200 m height and solar fields with radius up to 1-1.5 km. Ray-tracing and plant performance models usually implement the atmospheric attenuation as a third order polynomial function of the slant range. The models traditionally included in these tools have used a very simple approach considering only two extreme atmospheric conditions (very clear with high visibility of over 20 km, or very hazy atmosphere with visibility in the range of 5 km). This approach does not allow for dynamic estimation of the atmospheric attenuation according to the variable dynamics of the atmospheric conditions. In the PRESOL project a polynomial model was developed by fitting the results of multiple radiative transfer calculations covering a wide range of AOD conditions. The Polo's model thus allows easy implementation in ray-tracing and performance tools (since it is formulated as a third order polynomial), and also sensitivity to variable atmospheric conditions due to the dependence of AOD as input parameter to the model.

An accurate and reliable measuring system is used at PSA for continuous monitoring, started in summer 2017, the extinction coefficient and thus the atmospheric attenuation at a slant path of 742 m. The long experimental database is now very suitable for evaluating the performance of models for estimating the atmospheric attenuation. Therefore, in this work an assessment of Polo's model performance has been made and analyzed in aggregated hourly, daily and monthly means of atmospheric attenuation.

Polo's model performance has shown an agreement in the trend (inter and intra-annual) and variability of atmospheric attenuation but also a bias resulting in a general underestimation of the attenuation measured. In addition, the dispersion of Polo's model performance assessment is 10.9% in terms of RMSE. In the literature, there are several studies on the vertical profile of the aerosols in the atmosphere that remark differences in the near-surface aerosol extinction and vertical column extinction characterized by the AOD. Nevertheless, they also point out the correlation between both extinction parameters. Based on that studies and information in this work a correction method is proposed using the characteristics of the distribution function of observational values of the attenuation. The methodology for correcting Polo's model, denoted as quantile mapping, has allowed to fit a correction factor by piecewise exponential functions of the AOD. The new proposed model, i.e. the corrected version of Polo's model, has shown an unbiased performance and much higher accuracy, with 6.1% of RMSE for the hourly estimations of the attenuation. The correction factor developed improves the capability of modeling near surface extinction using as input the AOD (a parameter that integrates the extinction over the vertical column) keeping the polynomial formulation that make easier the implementation of this model in currently used tools for both performance and ray-tracing computation. The use of AOD as input parameter to the model (in addition to the slant range) confers universality and competence to the model since AOD information is available worldwide at different spatial and temporal resolutions from sun photometer ground stations, satellite-derived algorithms and reanalysis-based models.

Finally, it should be remarked that a model for estimating the near surface extinction coefficient as a function of the AOD could have been developed likewise; that approach has even more physical meaning. Attenuation has an exponential decreasing dependence with the extinction coefficient by the Lambert-Beer law. However, the formulation of Polo's models in terms of polynomial functions of the slant range was selected to easy its use and implementation in modeling tools for designing the solar field and for estimating the power output of solar tower plants. The new version of the Polo's model will be further evaluated in the future as long as new experimental data is available.

Acknowledgements

The authors would like to thank the PRESOL project (Ref. ENE2014-59454-C3-3-R), which is funded by the Ministerio de Economía y Competitividad (MINECO), and co-financed by the European Regional Development Fund. The authors wish also to thank and acknowledge the work being done by Dr. Stefan Wilbert and his team in operating and maintaining the Tabernas_PSA-DLR AERONET station, whose AOD data have been used in this work. Finally, we wish to recognize the effort in several topics of solar resource knowledge by the experts group

of IEA-PVPS Task 16, where atmospheric attenuation is included; fruitful discussions and collaborations have taken place by experts in the group and the corresponding author.

References

[1] Collado FJ, Guallar J. A review of optimized design layouts for solar power tower plants with campo code. Renewable and Sustainable Energy Reviews 2013;20:142–54. doi:10.1016/j.rser.2012.11.076.

[2] Wei X, Lu Z, Wang Z, Yu W, Zhang H, Yao Z. A new method for the design of the heliostat field layout for solar tower power plant. Renewable Energy 2010;35:1970–5. doi:10.1016/j.renene.2010.01.026.

[3] Luo Y, Lu T, Du X. Novel optimization design strategy for solar power tower plants. Energy Conversion and Management 2018;177:682–92. doi:10.1016/j.enconman.2018.09.089.

[4] Chen R, Rao Z, Liao S. Determination of key parameters for sizing the heliostat field and thermal energy storage in solar tower power plants. Energy Conversion and Management 2018;177:385–94. doi:10.1016/j.enconman.2018.09.065.

[5] Ballestrín J, Marzo A. Solar radiation attenuation in solar tower plants. Solar Energy 2012;86:388–92. doi:10.1016/j.solener.2011.10.010.

[6] Ballestrín J, Monterreal R, Carra ME, Fernández-Reche J, Polo J, Enrique R, et al. Solar extinction measurement system based on digital cameras. Application to solar tower plants. Renewable Energy 2018;125:648–54. doi:10.1016/j.renene.2018.03.004.

[7] Hanrieder N, Wilbert S, Pitz-Paal R, Emde C, Gasteiger J, Mayer B, et al. Atmospheric extinction in solar tower plants: Absorption and broadband correction for MOR measurements. Atmospheric Measurement Techniques 2015;8:3467–80. doi:10.5194/amt-8-3467-2015.

[8] Sánchez M, Fernández-peruchena CM, Bernardos A, Chueca R, Salinas I. High-Accuracy Real-time Monitoring of Solar Radiation Attenuation in Commercial Solar Towers. SolarPACES 2018, Casablanca October 2-5, 2018, Morocco: 2018.

[9] Hanrieder N, Wehringer F, Wilbert S, Wolfertstetter F, Pitz-Paal R, Campos VQ, et al. Determination of Beam Attenuation in Tower Plants. SolarPACES, vol. 11, 2012, p. 2012.

[10] Ballestrín J, Carra E, Monterreal R, Enrique R, Polo J, Fernández-Reche J, et al. One year of solar extinction measurements at Plataforma Solar de Almería. Application to solar tower plants. Renewable Energy 2019;136:1002–11. doi:10.1016/j.renene.2019.01.064.

[11] Carra E, Marzo A, Ballestrín J, Polo J, Barbero J, Alonso-Montesinos J, et al. Atmospheric extinction levels of solar radiation using aerosol optical thickness satellite data. Validation methodology with measurement system. Renewable Energy 2020;149:1120–32. doi:10.1016/j.renene.2019.10.106.

[12] Elias T, Ramon D, Brau J, Moulana M. Sensitivity of the Solar Resource in Solar Tower Plants to Aerosols and Water Vapor. SolarPACES 2018, Casablanca October 2-5, 2018, Morocco: 2018.

[13] Hanrieder N, Sengupta M, Xie Y, Wilbert S, Pitz-Paal R. Modeling beam attenuation in

solar tower plants using common DNI measurements. Solar Energy 2016;129:244–55. doi:10.1016/j.solener.2016.01.051.

[14] Polo J, Ballestrín J, Carra E. Sensitivity study for modelling atmospheric attenuation of solar radiation with radiative transfer models and the impact in solar tower plant production. Solar Energy 2016;134:219–27. doi:10.1016/j.solener.2016.04.050.

[15] Polo J, Ballestrín J, Alonso-Montesinos J, López-Rodriguez G, Barbero J, Carra E, et al. Analysis of solar tower plant performance influenced by atmospheric attenuation at different temporal resolutions related to aerosol optical depth. Solar Energy 2017;157:803–10. doi:10.1016/j.solener.2017.09.003.

[16] Sengupta M, Wagner M, Sengupta M, Wagner M. Estimating atmospheric attenuation in central receiver systems. SunShot Symposium. ASME 2012, 6th International Conference on Energy Sustainability. San Diego, CA, July 23-26; 2012, p. 1–5.

[17] Tahboub Z, Oumbe A, Hassar Z, Obaidli A. Modeling of Irradiance Attenuation from a Heliostat to the Receiver of a Solar Central Tower. Energy Procedia 2014;49:2405–13. doi:10.1016/j.egypro.2014.03.255.

[18] Hanrieder N, Wilbert S, Mancera-Guevara D, Buck R, Giuliano S, Pitz-Paal R. Atmospheric extinction in solar tower plants - A review. Solar Energy 2017;152:193–207. doi:10.1016/j.solener.2017.01.013.

[19] Ballestrín J, Carra ME, Enrique R, Monterreal R, Fernández-Reche J, Polo J, et al. Diagnosis of a lambertian target in solar context. Measurement 2018;119:265–9. doi:10.1016/J.MEASUREMENT.2018.01.046.

[20] Holben BN, Eck TF, Slutsker I, Tanre D, Buis JP, Setzer A, et al. AERONET : A federated instrument network and Data archive for aerosol characterization. Remote Sensing of Environment 1998;66:1–16.

[21] Holben BN, Tanré D, Smirnov A, Eck TF, Slutsker I, Abuhassan N, et al. An emerging ground-based aerosol climatology: Aerosol optical depth from AERONET. Journal of Geophysical Research: Atmospheres 2001;106:12067–97. doi:10.1029/2001JD900014.

[22] O'Neill NT, Eck TF, Smirnov A, Holben BN, Thulasiraman S. Spectral discrimination of coarse and fine mode optical depth. Journal of Geophysical Research D: Atmospheres 2003;108. doi:10.1029/2002jd002975.

[23] Giles DM, Sinyuk A, Sorokin MG, Schafer JS, Smirnov A, Slutsker I, et al. Advancements in the Aerosol Robotic Network (AERONET) Version 3 database - Automated near-real-time quality control algorithm with improved cloud screening for Sun photometer aerosol optical depth (AOD) measurements. Atmospheric Measurement Techniques 2019;12:169–209. doi:10.5194/amt-12-169-2019.

[24] Eck TF, Holben BN, Reid JS, Dubovik O, Smirnov A, O'Neill NT, et al. Wavelength dependence of the optical depth of biomass burning, urban, and desert dust aerosols. Journal of Geophysical Research Atmospheres 1999;104:31333–49. doi:10.1029/1999JD900923.

[25] Schuster GL, Dubovik O, Holben BN. Angstrom exponent and bimodal aerosol size distributions. Journal of Geophysical Research Atmospheres 2006;111:1–14. doi:10.1029/2005JD006328.

[26] Emde C, Buras-Schnell R, Kylling A, Mayer B, Gasteiger J, Hamann U, et al. The libRadtran software package for radiative transfer calculations (version 2.0.1) 2016;9:1647–72. doi:10.5194/gmd-9-1647-2016.

[27] Emde C, Buras-Schnell R, Kylling A, Mayer B, Gasteiger J, Hamann U, et al. The libRadtran software package for radiative transfer calculations (Version 2.0). Geosci Model Dev Discuss 2015;8:10237–303. doi:10.5194/gmdd-8-10237-2015.

[28] Mayer B, Kylling A, Emde C, Buras R. libRadtran user ' s guide 2015.

[29] Kistler BL. A user's manual for DELSOL3: A computer code for calculating the optical performance and optimal system design for solar thermal central receiver plants. Other Information: Portions of This Document Are Illegible in Microfiche Products Original Copy Available until Stock Is Exhausted Includes 5 Sheets of 48x Reduction Microfiche 1986:Medium: X; Size: Pages: 231. doi:SAND86-8018.

[30] Vittitoe CN, Biggs F. Terrestrial Propagation LOSS, presented Amer. Sec. ISES meeting. Sandia Report SAND78-1137C: 1978.

[31] Leary PL, Hankins JD. User's Guide for MIRVAL – A Computer Coe for Modeling the Optical Behavior of Reflecting Solar Concentrators. Sandia Report, SAND77-8280 , Alburquerque, USA 1979.

[32] Garcia P, Ferriere A, Bezian J-J. Codes for solar flux calculation dedicated to central receiver system applications: A comparative review. Solar Energy 2008;82:189–97. doi:10.1016/j.solener.2007.08.004.

[33] He Q, Li C, Mao J, Lau AKH, Chu DA. Analysis of aerosol vertical distribution and variability in Hong Kong. Journal of Geophysical Research Atmospheres 2008;113:D14211. doi:10.1029/2008JD009778.

[34] He Q, Li C, Geng F, Zhou G, Gao W, Yu W, et al. A parameterization scheme of aerosol vertical distribution for surface-level visibility retrieval from satellite remote sensing. Remote Sensing of Environment 2016;181:1–13. doi:10.1016/j.rse.2016.03.016.

[35] Chauvigné A, Sellegri K, Hervo M, Montoux N, Freville P, Goloub P. Comparison of the aerosol optical properties and size distribution retrieved by sun photometer with in situ measurements at midlatitude. Atmospheric Measurement Techniques 2016;9:4569–85. doi:10.5194/amt-9-4569-2016.

[36] Wang L, Lyu B, Deng Z, Liu J, Bai Y. Improving the estimating accuracy of extinction coefficient of surface aerosol with a new layer-resolved model in China. Science of the Total Environment 2020;713. doi:10.1016/j.scitotenv.2019.136443.

[37] Déqué M, Rowell DP, Lüthi D, Giorgi F, Christensen JH, Rockel B, et al. An intercomparison of regional climate simulations for Europe: assessing uncertainties in model projections. Climatic Change 2007;81:53–70. doi:10.1007/s10584-006-9228-x.

[38] Feigenwinter I, Kotlarski S, Casanueva A, Fischer AM, Schwierz C, Liniger MA. Exploring quantile mapping as a tool to produce user-tailored climate scenarios for Switzerland. Technical Report MeteoSwiss, 270, 44 Pp 2018;270.

[39] Piani C, Haerter JO, Coppola E. Statistical bias correction for daily precipitation in regional climate models over Europe. Theoretical and Applied Climatology 2010;99:187–92. doi:10.1007/s00704-009-0134-9.

[40] Themeßl MJ, Gobiet A, Heinrich G. Empirical-statistical downscaling and error correction of regional climate models and its impact on the climate change signal. Climatic Change 2012;112:449–68. doi:10.1007/s10584-011-0224-4.

[41] Polo J, Fernández-Peruchena C, Salamalikis V, Mazorra-Aguiar L, Turpin M, Martín-Pomares L, et al. Benchmarking on improvement and site-adaptation techniques for modeled solar radiation datasets. Solar Energy 2020;201:469–79. doi:10.1016/j.solener.2020.03.040.

[42] Blair N, Diorio N, Freeman J, Gilman P, Janzou S, Neises T, et al. System Advisor Model (SAM) General Description (Version 2017.9.5). Golden (CO): 2018. doi:10.1111/j.1532-5415.2009.02342.x.

[43] Neises T, Wagner MJ. Simulation of Direct Steam Power Tower Concentrated Solar Plant. ASME 2012 6th International Conference on Energy Sustainability, Parts A and B, 2012, p. 499. doi:10.1115/ES2012-91364.

[44] Gertig C, Delgado A, Hidalgo C, Ron R. SoFiA - A novel simulation tool for Central Receiver Systems. Energy Procedia 2014;49:1361–70. doi:10.1016/j.egypro.2014.03.145.